Dyes and Pigments 98 (2013) 195–200

Contents lists available at SciVerse ScienceDirect

Dyes and Pigments

journal homepage: www.elsevier.com/locate/dyepig

A highly selective copper fluorescent indicator based on aminoquinoline substituted BODIPY

Xu Jia, Xiaoting Yu, Xiaolong Yang, Jie Cui, Xiaoliang Tang, Weisheng Liu, Wenwu Qin*

Key Laboratory of Nonferrous Metal Chemistry and Resources Utilization of Gansu Province and State Key Laboratory of Applied Organic Chemistry, College of Chemistry and Chemical Engineering, Lanzhou University, Lanzhou 730000, PR China

ARTICLE INFO

Article history:
Received 23 December 2012
Received in revised form
16 February 2013
Accepted 19 February 2013
Available online 5 March 2013

Keywords:
Aminoquinoline
Copper probe
Bathochromic shifts
Time-resolved fluorescence
C–C bond cleavage
BODIPY

ABSTRACT

A highly selective fluorescent indicator for copper, substituted with an aminoquinoline group at the position 3 or 5 of the BODIPY has been synthesized. The indicator has very low fluorescence quantum yield in acetonitrile with emission maxima at 580 nm. Upon binding copper it shows 50 nm bathochromic shifts with a change of solution color and a large increase in the fluorescence intensity. The fluorescence lifetime in acetonitrile was too short and could not be determined; whereas fluorescence decay profile of the copper complex was described by a mono-exponential decay with the lifetime of 4.38 ns. ESI-MS enabled detection of a Cu·**1** CN complexes which was fromed by C–C bond cleavage of acetonitrile.

1. Introduction

Fluorescence spectroscopy is an attractive analytical technique to measure intracellular concentrations of biologically important ions and molecules. The design and development of fluorescent chemosensors for the detection of analytically important species is still an expanding area of research [1–3] Because of their excellent photophysical characteristics and easy synthesis, 4,4-difluoro-4-bora-3a,4a-diaza-*s*-indacene [4,5] (better known as BODIPY, difluoro*bo*ron *dipy*rromethene) derivatives are favored fluorophores in the design of fluorescent probes.

Hu et al. reported synthesis of three new 8-aminoquinoline-5-azo derivatives, which were found to be good fluorescence reagents for the determination of Cu^{2+} in ultraviolet region [6]. Since Cu^{2+} is a notorious fluorescence quencher, very few ratiometric fluorescent chemosensors for Cu^{2+} are available in the literature [7]. Therefore, the rapid monitoring of Cu^{2+}, especial the ratiometric and colorimetric detection, is very important. The first fluorescent chemosensor for Cu^{2+} based on the BODIPY as a reporter subunit (K_d = 3 μM) was published in 2006 [8a]. It had 8-hydroxyquinoline moiety as a receptor and showed significant fluorescence quenching in the presence of Cu^{2+} and Hg^{2+} with markedly higher selectivity for Cu^{2+}. Later, some good fluorescent chemosensors for Cu^{2+} based on the BODIPY were also reported [8b,c].

In a recent paper [9,10], we described the photophysical properties of the nonsymmetric 3-phenylamino and the symmetric 3,5-diphenylamino-substituted difluoroboron dipyrromethene dye. They showed some special spectroscopic properties that previous BODIPY derivatives did not have. Unlike BODIPY analogs with a 4-*N*,*N*-dimethylaminophenyl substituent at the *meso*-position [11,12], red-shifted, solvent polarity-dependent broad fluorescence band originating from an intramolecular charge transfer state (ICT) was not found in the emission spectrum of these aminophenyl-substituted BODIPY dyes. Moreover, there is a large difference in photophysical properties between the mono and bis-substituted aminophenyl BODIPY derivative. This means that spectroscopic properties of these BODIPY derivatives are mainly effected by the aminophenyl group at the 3- (and 5-) position(s). Consequently, one can expect that replacement of the aminophenyl group by other chelator having similar structure, would introduce a pronounced change of both absorption and emission maxima due to change of the properties upon complexation. Therefore, we synthesized a new BODIPY derivative **1** (Scheme 1) with the aminoquinoline attached via the N atom at the position 3 or 5 of the BODIPY moiety.

In this paper, we investigate the photophysical properties of new BODIPY derivative in a variety of solvents and its copper

* Corresponding author. Tel./fax: +86 931 8912582.
E-mail address: qinww@lzu.edu.cn (W. Qin).

0143-7208/$ – see front matter © 2013 Elsevier Ltd. All rights reserved.
http://dx.doi.org/10.1016/j.dyepig.2013.02.013

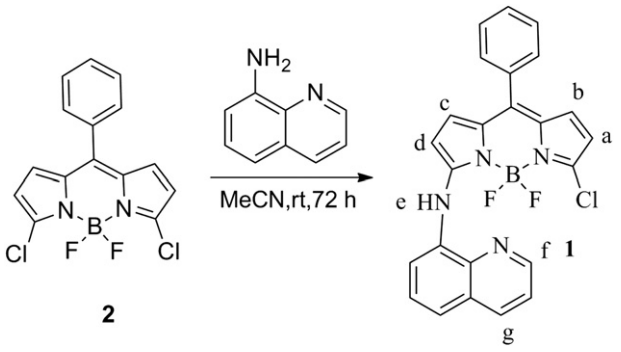

Scheme 1. Synthesis of sensor **1**.

complex in acetonitrile, using UV/Vis absorption and steady-state and time-resolved fluorescence techniques.

2. Experimental section

2.1. Instrument and reagent

All solvents (Aldrich, Sigma–Aldrich, Acros, or Riedel-Dehaën) were reagent grade quality and were used without further purification. ^{1}H and ^{13}C NMR spectra were taken on a Bruker DRX-400 and DRX-400/4 spectrometer with TMS as an internal standard and $CDCl_3$ as solvent. Chemical shift multiplicities are reported as s = singlet, d = doublet, and m = multiplet. ^{13}C spectra were referenced to the $CDCl_3$ (77.67 ppm) signal. Mass spectra were recorded in E.I. mode. Melting points were taken on an X-4 precise micro melting point cryoscope (Beijing Fukai Instrument Co.) and are uncorrected.

2.2. The synthesis of sensor *1*

Compound **2** was synthesized as described previously [13]. 50 mg (0.15 mmol) of compound **2** was dissolved in 20 mL acetonitrile, 20 mg (0.14 mmol) of 8-aminoquinoline was added to it. The reaction mixture was stirred at room temperature for 72 h. After solvent was remove by under reduced pressure, the crude solid was purified by column chromatography on silica purified through column chromatography over silica with ethyl acetate and petroleum ether (1:4) to obtain 37 mg of **1** in 60% of yield [13,14]. Reddish solid, mp 62–64 °C. ^{1}H NMR ($CDCl_3$, 400 MHz) δ 6.27 (d, 1H, J = 4.0 Hz, H-a), 6.46 (d, 1H, J = 4.0 Hz, H-b), 6.83 (d, 1H, J = 4.0 Hz, H-c), 6.96 (d, 1H, J = 4.0 Hz, H-d), 7.44–7.53 (m, 9H), 8.12 (d, 1H, J = 8.0 Hz, H-g), 8.92 (s, 1H, H-f), 10.52 (s, 1H, H-e); ^{13}C NMR ($CDCl_3$, 100 MHz): δ111.83, 113.65, 114.75, 122.30, 122.65, 126.39, 128.23, 128.40, 129.45, 130.28, 132.17, 133.56, 134.27, 135.52, 135.93, 149.35, 156.73. MS (ESI) m/z calcd. For $C_{24}H_{16}BClF_2N_4$ 444.1; found 445.1 (M+1); 425.3 (M-F, 100%).

2.3. Crystal structure determination

Crystals of **1** were obtained by slow evaporation of the ethyl acetate in air over two weeks, yielding red stick crystals with approximate dimensions of 0.18 × 0.18 × 0.20 mm^3 suitable for X-ray diffraction. The crystals belonged to the monoclinic space group P-1 (number 2) with cell dimensions a = 7.596(3) Å, b = 8.866(4) Å, c = 15.385(7) Å, α = 79.944(5)°, β = 84.348(5)°, γ = 88.261(5)°, V = 1015.1(7) Å^3, Z = 2 ρ_{calc} = 1.455 g cm^{-3}, $2\theta_{max}$ = 50.00°, μ(Mo$K\alpha$) = 0.227 mm^{-1}.

The data for **1** was measured on a Bruker Smart APEX II CCD diffractometer at 296 ± 2 K equipped with graphite-monochromatized Mo $K\alpha$ radiation (λ = 0.71073 Å). The structures were solved by direct methods. All non-hydrogen atoms were subjected to anisotropic refinement by full-matrix least-squares methods on F^2 by using the program package SHELXS-97 [15]. Hydrogen atoms were placed at calculated positions. Final R indices [$I > 2\sigma(I)$] were R_1 = 0.0758, wR_2 = 0.1939; max./min. residual electron density 0.42/−0.31 e$^-$ Å^{-3}.

Crystallographic data (excluding structure factors) for the structure reported in this paper have been deposited with the Cambridge Crystallographic Data Centre as supplementary publication no. CCDC 825211 for **1**. Copies of the data can be obtained free of charge on application to CCDC, 12 Union Road, Cambridge CB2 1EZ, U.K. (fax: +44(0)-1223-336033 or e-mail: deposit@ccdc.cam.ac.uk or www.ccdc.cam.ac.uk/conts/retrieving.html).

2.4. Steady-state UV–vis absorption and fluorescence spectroscopy

UV–vis absorption spectra were recorded on a Varian UV-Cary100 spectrophotometer and for the corrected steady-state excitation and emission spectra, a Hitachi F-4500 spectrofluorometer was employed. Freshly prepared samples in 1-cm quartz cells were used to perform all UV–vis absorption and emission measurements. For the determination of the fluorescence quantum yields ϕ_f of **1**, only dilute solutions with an absorbance below 0.1 at the excitation wavelength (λ_{ex} = 488 or 500 nm) were used. Rhodamine 6G in water (ϕ_f = 0.76) was used as fluorescence standard [16]. The ϕ_f values reported in this work are the averages of multiple independent measurements. The majority of the ϕ_f determinations were done using undegassed samples. In all cases, correction for the solvent refractive index was applied. All spectra were recorded at 20 °C using undegassed samples. To check the influence of dissolved O_2 on ϕ_f, some samples were purged with nitrogen for 15 min prior to measurement. The obtained ϕ_f values were within experimental error equal for aerated and degassed samples. The titration experiments with copper were carried out by adding small quantities of a stock solution of metal perchlorate salts in MeCN to a much larger volume (25 mL) of solutions of **1**.

2.5. Copper binding properties

The ground-state dissociation constants K_d of the complexes between Cu^{2+} and the probes were determined in an acetonitrile solution by fluorometric titration as a function of Cu^{2+} concentration using the fluorescence excitation and/or emission spectra. Nonlinear fitting of Eq. (1) [17] to the steady-state fluorescence data F recorded as a function of [Cu^{2+}] yields values of K_d, the fluorescence signals F_{min} and F_{max} at minimal and maximal [Cu^{2+}], respectively (corresponding to the free and Cu^{2+} bound forms of the probe, respectively), and n (the number of copper ions bound per probe). Equation (1) assumes that the absorbance of the sample is small (<0.1) and that Cu^{2+} complex formation in the excited state is negligible.

$$F = \frac{F_{max}\left[Cu^{2+}\right]^n + F_{min}K_d}{K_d + \left[Cu^{2+}\right]^n} \quad (1)$$

Fitting Eq. (1) to the steady-state fluorescence data F with n, K_d, F_{min}, and F_{max} as freely adjustable parameters always gave values of n close to 1 (n = 1.06–1.30 in this experiment), indicating that one copper ion is bound per fluorescent indicator. Therefore, n was kept fixed at 1 in the final fittings of Eq. (1) to the fluorescence excitation or emission spectral data, from which the estimated values of K_d, F_{min}, and F_{max} are reported.

Since large spectral shifts are observed in the absorption spectra of **1**, the *ratiometric* method can be used to estimate the ground-state dissociation constants K_d (Eq. (2)).

$$R = \frac{R_{max}[Cu^{2+}]^n + R_{min}K_d\xi}{K_d\xi[Cu^{2+}]^n} \quad (2)$$

$R = A(\lambda^1_{abs})/A(\lambda^2_{abs})$ is the ratio of the absorbances at the two indicated wavelengths. Nonlinear fitting of Eq. (2) to the absorption ratiometric data R recorded as a function of $[Cu^{2+}]$ yields values of K_d, the ratios R_{min} and R_{max} at minimal and maximal $[Cu^{2+}]$, respectively (corresponding to the free and complex forms of the copper probe, respectively), and n. Since $\xi = A_{min}(\lambda^2_{abs})/A_{max}(\lambda^2_{abs})$ – the ratio of the absorbances at the indicated wavelength – is experimentally accessible, a value for K_d can be extracted from ratiometric absorption data.

2.6. Time-resolved fluorescence spectroscopy

Fluorescence lifetimes were measured by a FLS920 at room temperature. The samples were dissolved in CH_3CN and the concentrations were adjusted to have optical densities at the excitation wavelength <0.1. Solutions were purged with nitrogen for 15 min prior to analysis. The monitored wavelength was 580 nm and 590 nm for **1** in solvents when excite the samples at 490 nm. For the copper complex, the monitored wavelength was from 580 nm to 630 nm when excited at 570 nm.

Fluorescence decay histograms were obtained on an Edinburgh instrument FLS920 spectrometer equipped with a supercontinue white laser (400–700 nm), using the time-correlated single photon counting technique in 2048 channels. Histograms of the instrument response functions (using a LUDOX scatterer) and sample decays were recorded until they typically reached 5×10^3 counts in the peak channel. Obtained histograms were fitted as sums of the exponential, using Gaussian-weighted nonlinear least squares fitting based on Marquardt–Levenberg minimization implemented in the software package of the instrument. The fitting parameters (decay times and preexponential factors) were determined by minimizing the reduced chi-square χ^2. An additional graphical method was used to judge the quality of the fit that included plots of surfaces ("carpets") of the weighted residuals versus channel number. All curve fittings presented here had χ^2 values below 1.1.

All measurements were done at 20 °C.

3. Result and discussion

3.1. Crystal structure of *1*

As shown in Fig. 1, in the BODIPY ring system, the two planar pyrrole subunits and the boron atom constitute a plane for which the deviation of all non-hydrogen atoms is within the 0.005–0.070 Å range. The angle between the two pyrrole moieties is 4.41°, which is near the average 6.5° (range 0°–18.1°) found in the Cambridge Structural Database (CSD, updated to October 2008). The two fluorine atoms are equidistant above and under the plane of the pyrrole moieties, and the F–B–F plane is 109.86° to the plane of the BODIPY core. However, the phenyl ring at the *meso*-position, the aminoquinoline ring and the pyrrole rings are not coplanar. The phenyl ring at the *meso*-position makes an angle of 59.04° with the BODIPY plane, which is in the range of most BODIPY derivatives (40.3°–90°), but is smaller than the average value of 76.4° found in the CSD. The dihedral angles between aminoquinoline ring and pyrroles is 33.09°.

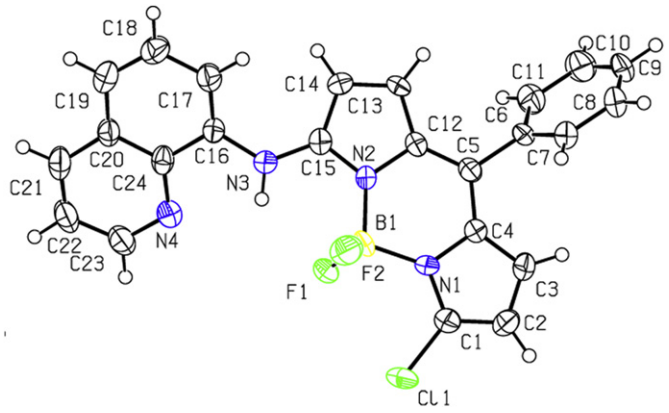

Fig. 1. ORTEP representation of compound **1** with displacement ellipsoids at the 20% probability level.

3.2. Spectroscopic properties

The absorption and emission spectra of molecule **1** were recorded in several solvents (Fig. 2). The absorption spectrum is of comparable shape as those of the described BODIPY dyes [18,19], with an intense absorption band somewhat above 560 nm and a less pronounced shoulder at shorter wavelengths. The absorption spectra of **1** in toluene and chloroform are analogous to that in cyclohexane and they all show two absorption bands: the 0–0 band of a strong S_0–S_1 transition with a maximum ranging at 560 nm and a more pronounced shoulder on the high-energy side. The absorption spectra are affected by solvent polarity; the maximum being blue-shifted (by ~40 nm) when the solvent is changed from cyclohexane (560 nm) to acetonitrile (518 nm). Additionally, a weaker, broad absorption band is found in the UV at around 350 nm. This broader and weaker absorption band is attributed to the S_0–S_2 transition.

Compound **1** in cyclohexane shows an emission spectrum with a maximum at ~580 nm, displaying the typical emission features of BODIPY. The maximum of the fluorescence band isn't affected by solvent polarity. Contrary to the near-invariance of the emission wavelength maximum $\lambda_{em}(max)$ in solvent. The fluorescence quantum yield ϕ_f of **1** is strongly solvent dependent. The ϕ_f values are moderately high in cyclohexane (0.17), somewhat lower in toluene (0.04), while in all other solvents of higher polarity the emission intensity is strongly quenched ($\phi_f = 0.01$ in $CHCl_3$ and 0.0024 in MeCN). The low ϕ_f value for **1** in polar solvents can be attributed to an efficient quenching via an excited-state ICT process

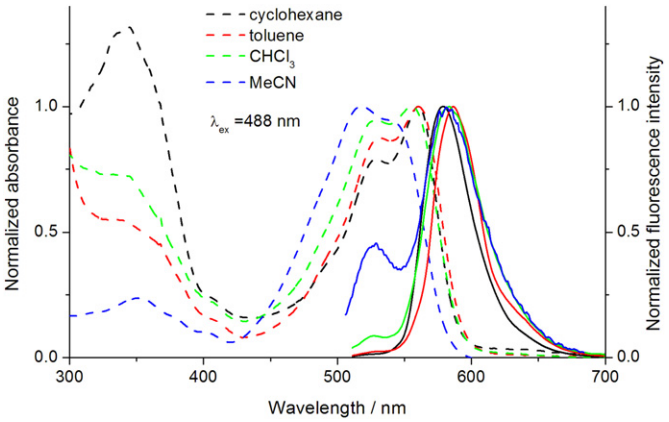

Fig. 2. Normalized absorbance (dash curves) and fluorescence emission (solid curves) spectra of **1** in several solvents.

from the nitrogen atom of the aminoquinoline amine NH moiety to the strongly electron deficient BODIPY acceptor. As the solvent polarity increases, ICT becomes more favored, which induces the quenching of fluorescence and shifting of spectra. The solvent dependence of ϕ_f may be interpreted as an indication of a small contribution of a dipolar resonance state to the ground or excited state of **1** [10]. The blue shift of the absorption spectrum from cyclohexane to MeCN suggests that the increase of the electron density in the conjugated BODIPY system by the aminoquinoline moiety is less pronounced in the excited state than in the ground state.

3.3. Spectroscopic properties of **1** with Cu^{2+}

The changes in optical properties induced by addition of metal ions perchlorates to acetonitrile solutions of **1** are shown in Fig. 3. While the fluorescence emission spectra of **1** are hardly altered in the presence of other metal ions, pronounced changes are observed upon addition of Cu^{2+} ions. The addition of Cu^{2+} to a solution of **1** in CH_3CN strongly affects the absorption spectra. Upon increasing the metal ion concentration, the lowest energy absorption band (with maximum at 518 and 547 nm in the absence of metal ions) decreases in intensity whereas a new peak appears at approximately 610 nm whose intensity increases with higher metal ion concentration The change in the absorption spectra causes the immediate change of the solution color from red to violet, which can be

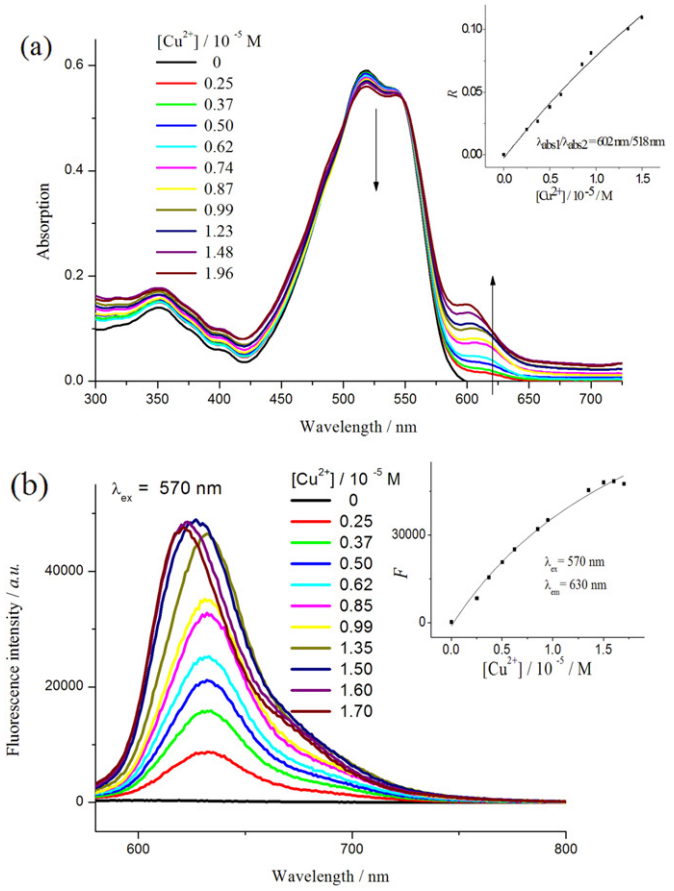

Fig. 3. Absorption spectra (a) and fluorescence emission spectra ($\lambda_{ex} = 570$ nm) (b) of **1** (15 μM) in acetonitrile as a function of $[Cu^{2+}]$. The insets of (a) and (b) show the best fits to the *ratiometric* ($\lambda^1_{abs}/\lambda^2_{abs} = 602/518$ nm) absorption titration data (for a) and the *direct* ($\lambda_{ex} = 570$ nm, $\lambda_{em} = 630$ nm) fluorimetric emission titration data (for b) of **1** as a function of $[Cu^{2+}]$.

detected by the naked eye. The relative contributions of the 602/518 nm signals change with varying $[Cu^{2+}]$ and the vis absorption spectra show isosbestic points at 500 and 548 nm. The fluorescence emission spectra of **1** are shown as a function of $[Cu^{2+}]$ in Fig. 3b. The maximum of the fluorescence emission band shifts bathochromically from 580 nm in ion-free acetonitrile to 630 nm in the presence of Cu^{2+} and is accompanied by an increase in intensity. The excitation spectra (see Fig. S1) show an excitation maximum at 614 nm with increasing concentration of copper, implying that the fluorescence originates mainly from the excited state of the copper complex. The highest measured ϕ_f value (0.04 for excitation at 570 nm) is found at the copper ion concentration of 15 μM. Upon binding of Cu^{2+}, the electron-donating properties of the amine are reduced, partially suppressing the ICT effect, causing a red shift and an enhancement in the fluorophore's fluorescence intensity. Complex formation causes rotation of the aminoquinoline ring resulting in more extended planarity of the chromophore. Beside the ICT effect, it caused an enhancement in fluorophore's fluorescence intensity. In a previous paper, we have shown that the behavior of phenylamino substituted BODIPY dye is different from that observed in related BODIPY dyes, in which the amine donor group is separated from the BODIPY core by a styryl spacer. The aminoquinoline moiety plays the role of a donor in both the ground and excited state of **1**, which results in the appearance of a dipole pointing with its negative head toward the BODIPY core. The ground-state dipole moment in **1** is larger than the excited-state dipole moment so that the dipole moment difference points from the BODIPY to the aminoquinoline moiety. This is responsible for the negative solvatochromic effect observed for this dye: the ground-state absorption spectrum shows a large blue shift with increasing solvent polarity (the inertial contribution to the dielectric response stabilizes the ground state to a larger extent than the excited state, hence the blue shift). When the Cu^{2+} coordinated with the nitrogen atoms in the complex with **1**, the charge transfer **1** was blocked, causing a red shift in the fluorescence spectrum in acetonitrile solution (polar solvent). Consequently, the complex absorbs and fluoresces more intensely at longer wavelengths relative to the uncomplexed dye **1** [9] (Table 1).

The ground-state dissociation constants K_d of the complexes between Cu^{2+} and the probe were determined in acetonitrile solution by fluorimetric titration as a function of Cu^{2+} concentrations using the fluorescence excitation and/or emission spectra. The results obtained at $\lambda_{exc} = 570$ nm indicated a complex of 1:1 stoichiometry and yielded a value of 22 μM for the K_d. Since there is a large shift of the absorption spectra, the ratiometric absorption measurements could be performed. By using the ratio of decrease/increase in the absorption bands at $\lambda^1_{abs}/\lambda^2_{abs} = 602/518$ nm, the K_d value of 31 μM was determined. The K_d value of 22 μM obtained from direct fluorimetric titrations using emission spectra is in good agreement with that from (ratiometric) absorption measurements. This 1:1 stoichiometry binding mode was also supported by the data of Job's plots (Fig. S2). The detection limit was calculated based on the fluorescence titration. The emission intensity of **1** without Cu^{2+} was measured 10 times and the standard deviation of blank measurements was determined. A good linear relationship between the fluorescence intensity and the Cu^{2+} concentration could be obtained in the 0–15 μM concentration range ($R = 0.991$; Fig. S3). The detection limit was then calculated with the equation: detection limit $= 3\sigma/m$, where σ is the standard deviation of blank measurements, m is the slope between intensity versus sample concentration. The detection limit was measured to be 9.0×10^{-9} M.

Lu has reported C–C bond cleavage of acetonitrile by a dinuclear copper cryptate [20a], The dinuclear copper (II) cryptate $[Cu_2L](ClO_4)_4$ cleaves the C–C bond of acetonitrile at room temperature to

Table 1
Photophysical data of **1** in different solvents, and in the presence of copper ion in acetonitrile. K_d is the average value determined from all direct analyses of the fluorometric and spectrophotometric titrations.

Complex	Solvent	λ_{abs}(max)/nm	λ_{em}(max)/nm	Φ_f	τ/ns	$k_f/10^7\ S^{-1}$	K_d/μM
1	Cyclohexane	560	580	0.17	3.21	5.3	
	Toluene	561	586	0.04	0.82	4.9	
	Chloroform	555	583	0.01			
	Acetonitrile	518,547	580	0.0024			
1-Cu^{2+}	Acetonitrile	610	630	0.04	4.26 (610–630 nm)		22

produce a cyanide bridged complex of $[Cu_2L(CN)](ClO_4)_3\cdot 2CH_3CN\cdot 4H_2O$. Cleavage of the C–CN bond of acetonitrile with monomeric Cu^{2+} complex has also been observed before [20b,c]. In our experiment, the formation of Cu·**1** adduct was further confirmed by mass spectrometry. The electrospray ionization mass spectrum of the copper adducts with **1** showed a molecular mass of 619.4, (Fig. SI) which may be correspond to the formula of $[Cu\cdot\mathbf{1}(2CN)](H_2O\cdot CH_3CN)$, that is, the MS data suggest the presence of CN complexes. Thus, it might be possible that these species are formed upon ESI ionization.

The expected structural change of **1** in the presence of copper metal ions is depicted in Fig. 4. The detection system in this work was pure acetonitrile. The electrospray ionization mass spectrum conformed that the product of **1** and Cu^{2+} was formed from CH_3CN. When we change detection system to aqueous/MeOH systems, the probe doesn't show the high selectivity for Cu^{2+} anymore. Moreover, same as nonsymmetric 3-phenylamino and the symmetric 3,5-diphenylamino-substituted difluoroboron dipyrromethene dye, pH doesn't affect the response of the probe's fluorescence intensity.

Fluorescence decay traces of BODIPY derivative **1** and its copper complex were recorded at several emission wavelengths by the single-photon timing method [21]. Fluorescence decay profiles of **1** could be described by a single-exponential decay in cyclohexane and toluene. The lifetimes τ estimated via single curve analysis were independent of the observation wavelength. The lifetime is about 3.21 ns in cyclohexane and 0.82 ns in toluene.

From the decay traces displayed in Fig. 5 it is clear that the fluorescence lifetimes decrease with increasing solvent polarity (from toluene to acetonitrile).

The rate constant of radiative (k_f) and non-radiative (k_{nr}) deactivation can be calculated from the measured fluorescence quantum yield ϕ_f and the single-exponential fluorescence lifetime according to Eqs. (3) and (4):

$$k_f = \phi_f/\tau \tag{3}$$

$$k_{nr} = \left(1-\phi_f\right)/\tau \tag{4}$$

The values of k_f are $5.3\times10^7\ s^{-1}$ and $4.9\times10^7\ s^{-1}$, respectively, indicating that k_f is nearly independent of the low-polarity solvent used. The k_f values obtained for **1** are different when compared to those obtained from the common BODIPY compounds. The fluorescence lifetimes of **1** in acetonitrile and other polar solvents were too short and could not be determined. Upon complexation by Cu^{2+} in acetonitrile, in addition to the change of the solution color and the increase in fluorescence intensity, the fluorescence decay became slower.

Fig. 5b displays the fluorescence decay traces of **1** complex by Cu^{2+} in acetonitrile at $\lambda_{em} = 590$, $\lambda_{em} = 610$ and $\lambda_{em} = 630$ nm. The curve at 590 nm is a sum of two exponentials. At 590 nm, the contributions of the τ_1 (4.37 ns) and τ_2 (1.84 ns) components are 76% and 24%, respectively. The contribution from the τ_1 component increases, whereas that of the τ_2 component decreases with increasing emission wavelength (See Table S1). Above 610 nm, the fluorescence decays are single exponential with lifetime is 4.38 ± 0.02 ns, implying that the fluorescence emission wavelengths above 610 nm and the fluorescence excitation wavelengths

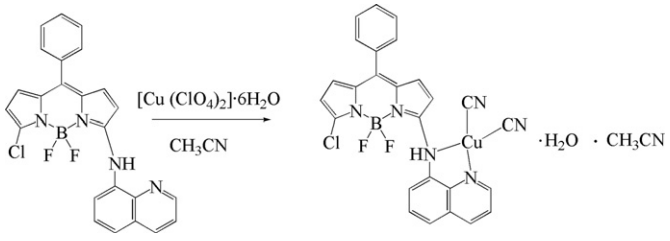

Fig. 4. Schematic representation of the proposed structure changed after bound with Cu^{2+} in acetonitrile.

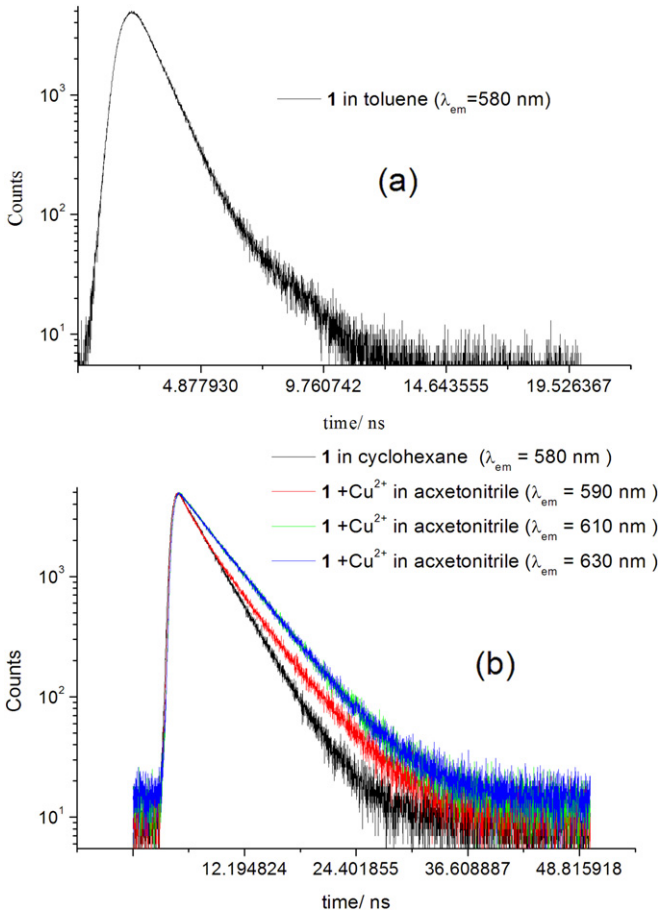

Fig. 5. Representative fluorescence decay curves of **1** in toluene (a) and in cyclohexane (b, black curve-λ_{em} = 580 nm) excited at 490 nm and **1** in acetonitrile in addition of copper ions (b, λ_{em} = 590–630 nm) excited at 570 nm at different time windows (20 ns and 50 ns, respectively).

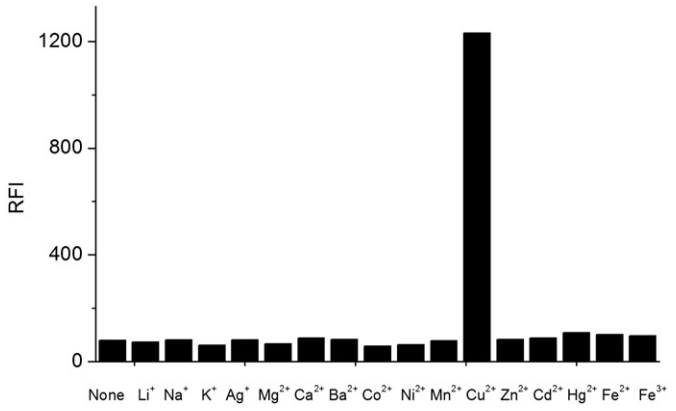

Fig. 6. Relative fluorescence intensity of the acetonitrile solution of **1** (15 μM) in the presence of various cations in the concentrations of 300 μM (for Cu^{2+} the concentration is 15 μM) in acetonitrile.

about 610 nm are mainly from the excited state of the copper complex.

It is known that achieving a high selectivity for the analyte of interest over a complex background of potentially competing species is a challenging task in sensor development. Fig. 6 illustrates the fluorescence response of **1** in the presence of copper and other metal ions. To further gauge selectivity for copper ion over other metal ions, the examination of metal/copper coexisted system was shown at Fig. S4.

Since the emission intensity of compound **1** almost does not change on addition of other metal ions, it means that the detection of Cu^{2+} by **1** is hardly affected by these common coexistent metal ions. The distance of two N atoms in aminoquinoline is 2.662 Å. In addition, the steric hindrance from two F atoms and the electrostatic repulsion between the chlorine and fluorine atoms made only copper ion fit well with aminoquinoline. The shift of the absorption and fluorescence spectra of **1** upon addition of Cu^{2+} is completely opposite to the intramolecular charge transfer (ICT) BODIPY potassium probe substituted with an aza crown ether at the position 3 [22].

4. Conclusion

We have synthesized the visible light excitable, fluorescent BODIPY-based dye **1**, which shows solvent-dependent spectroscopic/photophysical properties. The aminoquinoline substituted BODIPY dye forms 1:1 complexes with several transition-metal ions Cu^{2+}. The new boradiazaindacene dye is an example of a very high selectivity for fluorescent probe for copper metal ions displaying large absorption and fluorescence changes in an analytically interesting wavelength region.

Acknowledgments

W.Q. thanks the 'Program for New Century Excellent Talents in University' (NCET-09-0444), the Natural Science Foundation of China (No. 21271094) and the 'Fundamental Research Funds for the Central Universities' (lzujbky-2011-22) and the 'National Science Foundation for Fostering Talents in Basic Research of the National Natural Science Foundation of China' (Grant No. J1103307) and the 'International Cooperation Program of Gansu Province' (1104WCGA182). This study was supported in part by the 'Key Program of National Natural Science Foundation of China' (20931003).

Appendix A. Supplementary data

Supplementary data related to this article can be found at http://dx.doi.org/10.1016/j.dyepig.2013.02.013.

References

[1] (a) Desvergne JP, Czarnik AW. Chemosensors of ion and molecule recognition. Dordrecht, The Netherlands: Kluwer; 1997;
(b) Haugland RP. Handbook of fluorescent (probes and research chemicals. 9th ed. Eugene, OR, USA: Molecular Probes, Inc.; 2002.
[2] Haugland RP. The handbook. A guide to fluorescent probes and labeling technologies. 10th ed. Eugene, Oregon, USA: Molecular Probes, Inc.; 2005.
[3] Valeur B, Brochon JC. New trends in fluorescence spectroscopy. Applications to chemical and life sciences. Berlin: Springer; 2002.
[4] Treibs A, Kreuzer FH. Liebigs Ann Chem 1968;718:208–23.
[5] (a) Loudet A, Burgess K. Chem Rev 2007;107:4891–932;
(b) Ulrich G, Ziessel R, Harriman A. Angew Chem Int Ed 2008;47:1184–201.
[6] Cao Q, Wang K, Hu Z, Xu Q. Talanta 1998;47:921–7.
[7] (a) Mitchell KA, Brown RG, Yuan D, Chang SC, Utecht RE, Lewis DE. J Photochem Photobiol A Chem 1998;115:157–61;
(b) Xu Z, Xiao Y, Qian X, Cui J, Cui D. Org Lett 2005;7:889–92;
(c) Xu Z, Qian X, Cui J. Org Lett 2005;7:3029–32;
(d) Mashraqui S, Khan T, Sundaram S, Ghadigaonkar S. Tetrahedron Lett 2008;49:3739–43;
(e) Jiao L, Li J, Zhang S, Wei C, Hao E, Vicente M. New J Chem 2009;33:1888–93;
(f) Lin W, Yuan L, Tan W, Feng J, Long L. Chem Eur J 2009;15:1030–5;
(g) Zhou Y, Wang F, Kim Y, Kim S, Yoon J. Org Lett 2009;11:4442–5;
(h) Goswami S, Sen D, Das N. Org Lett 2010;12:856–9;
(i) Liu M, Zhao H, Quan X, Chen S, Yu H. Chem Commun 2010;46:1144–6;
(j) Xu Z, Yoon J, Spring D. Chem Commun 2010;46:2563–5;
(k) Chen X, Wang J, Cui J, Xu Z, Peng X. Tetrahedron 2011;67:4869–73.
[8] (a) Mei Y, Bentley PA, Wang W. Tetrahedron Lett 2006;47:2447–9;
(b) Qi X, Jun E, Xu L, Kim S, Hong J, Joon Y, et al. J Org Chem 2006;71:2881–4;
(c) Qi X, Kim S, Han S, Xu L, Lee A, Kim S, et al. Tetrahedron Lett 2008;49:261–4.
[9] Qin W, Leen V, Rohand T, Dehaen W, Dedecker P, Van der Auweraer M, et al. J Phys Chem A 2009;113:439–47.
[10] Qin W, Leen V, Dehaen W, Cui J, Xu C, Tang X, et al. J Phys Chem C 2009;113:11731–40.
[11] Qin W, Baruah M, Van der Auweraer M, De Schryver FC, Boens N. J Phys Chem A 2005;109:7371–84.
[12] Kollmannsberger M, Rurack K, Resch-Genger U, Daub J. J Phys Chem A 1998;102:10211–20.
[13] Baruah M, Qin W, Basarić N, De Borggraeve WM, Boens N. J Org Chem 2005;70:4152–7.
[14] Litter BJ, Miller MA, Hung CH, Wagner RW, O'Shea DF, Boyle PD, et al. J Org Chem 1999;64:1391–6.
[15] Sheldrick GM. SHELXS97 program for solution of crystal structure. Germany: University of Göttingen; 1997.
[16] Olmsted J. J Phys Chem 1979;83:2581.
[17] Cielen E, Tahri A, Ver Heyen K, Hoornaert GJ, De Schryver FC, Boens N. J Chem Soc Perkin Trans 2 1998:1573–80.
[18] (a) López Arbeloa T, López Arbeloa F, López Arbeloa I, García-Moreno I, Costela A, Sastre R, et al. Chem Phys Lett 1999;299:315–21;
(b) Costela A, García-Moreno I, Gomez C, Sastre R, Amat-Guerri F, Liras M, et al. J Phys Chem A 2002;106:7736–42;
(c) López Arbeloa F, Bañuelos Prieto J, Martínez Martínez V, Arbeloa López T, López Arbeloa I. Chem Phys Chem 2004;5:1762–71.
[19] Vos de Wael E, Pardoen JA, van Koeveringe JA, Lugtenburg J. Recl Trav Chim Pays Bas 1977;96:306–9.
[20] (a) Lu T, Zhuang X, Li Y, Chen S. J Am Chem Soc 2004;126:4760–1;
(b) Marlin D, Olmstead M, Mascharak P. Angew Chem Int Ed 2001;40:4752–4;
(c) Xu F, Huang W, Zeng X. Dalton Trans 2010;39:10652–8.
[21] Boens N, Qin W, Basarić N, Hofkens J, Ameloot M, Pouget J, et al. Anal Chem 2007;79:2137–49.
[22] Baruah M, Qin W, Vallée RAL, Beljonn D, Rohand T, Dehaen W, et al. Org Lett 2005;7:4377–80.